

Taylor & Francis
Taylor & Francis Group

Transactions of the Indian Ceramic Society

ISSN: 0371-750X (Print) 2165-5456 (Online) Journal homepage: https://www.tandfonline.com/loi/tcer20

Effect of Calcination on Microstructure Development and Properties of Hydroxyapatite Powders Extracted from Human and Bovine Bones

Kerim Emre Öksüz, Seyran Kilinç & Ali Özer

To cite this article: Kerim Emre Öksüz, Seyran Kilinç & Ali Özer (2019) Effect of Calcination on Microstructure Development and Properties of Hydroxyapatite Powders Extracted from Human and Bovine Bones, Transactions of the Indian Ceramic Society, 78:1, 41-45, DOI: 10.1080/0371750X.2019.1588170

To link to this article: https://doi.org/10.1080/0371750X.2019.1588170

Published online: 02 Apr 2019.

Submit your article to this journal

Article views: 20

View related articles

View Crossmark data

Full Terms & Conditions of access and use can be found at
https://www.tandfonline.com/action/journalInformation?journalCode=tcer20

Trans. Ind. Ceram. Soc., vol. 78, no. 1, pp. 41-45 (2019).
© 2019 Indian Ceramic Society
ISSN 0371-750X (Print), ISSN 2165-5456 (Online)
http://dx.doi.org/10.1080/0371750X.2019.1588170

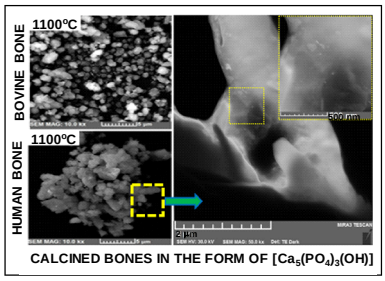
Effect of Calcination on Microstructure Development and Properties of Hydroxyapatite Powders Extracted from Human and Bovine Bones

Kerim Emre Öksüz,[1,*] Seyran Kilinç[2] and Ali Özer[1]

[1]Department of Metallurgical and Materials Engineering, Sivas Cumhuriyet University, Sivas – 58140, Turkey
[2]Department of Orthopedic and Traumatology, School of Medicine, Cumhuriyet University, Sivas – 58140, Turkey
[MS received June 26, 2018; Revised copy received October 24, 2018; Accepted February 22, 2019]

ABSTRACT

This study represents a comprehensive discussion of hydroxyapatite (HAp) formation from human and bovine bones. The phase formation and surface morphologies of prepared HAp powders were determined by XRD and SEM analyses, respectively. TEM was employed to understand the internal compositions with high magnifications and particle size. FT-IR characterizations provided information about molecular interactions and structures. In order to understand the effect of heat treatment at different temperatures and ultimately to get the desired morphology/particle size of the HAp powders derived from human and bovine, the powder samples were calcined at 700° to 1100°C with an interval of 100°C. At 700°C, the organic components were removed and finally, a carbonate apatite was obtained. The degree of crystallinity and crystallite size were noticed to increase progressively with calcination temperature. The overall results showed that the calcination temperature highly influenced the properties of HAp powders derived from human and bovine bone samples. As expected, higher temperatures led to more pure form of HAp with higher degree of crystallinity, larger crystallite size, and a less porous structure. Besides, the human bone structure, in contrary to the bovine bone, did not show temperature sensitivity by means of crystallite size increase.



[Keywords: Calcination, Hydroxyapatite, Chemical and structural properties]

Introduction

Although autografts are still the most preferred materials to replace human bone tissue, other alternatives are commonly used to overcome its drawbacks like limited supply and the requisite of additional surgery. The alternatives can be allografts, xenografts and synthetic biomaterials.[1–3] Each of these options has advantages and disadvantages. Allografts and xenografts, though currently being applied, can introduce the risk of rejection and disease transfer.[1, 2, 4] Synthetic hydroxyapatite minimizes these limitations, but it lacks osteoinductive properties and exhibits poor mechanical properties, especially when exposed to wet environments as interaction with body fluids.[2–6] Natural hydroxyapatite obtained in this way has the advantages of inheriting the chemical composition and structure of the raw material;[7–10] hence, can be an alternative solution for numerous applications based on its analogous synthetic products.

Hydroxyapatite (HAp), $Ca_{10}(PO_4)_6(OH)_2$, is similar to human hard tissues in morphology and composition.[11] Particularly, it has a hexagonal structure[12, 13] and a stoichiometric Ca/P ratio of 1.67, which is identical to bone apatite (Fig. 1a).[12, 14] An important characteristic of HAp is its stability when compared to other calcium phosphates. Thermodynamically, HAp is the most stable calcium phosphate compound under physiological conditions at room temperature, at neutral pH range of 5.5-7.4 (<5 mmol.L^{-1} Ca^{2+} ions and <60 mmol.L^{-1} PO_4^{3-} ions at ≈40°C) and emulsion suspended composition of the body fluids at neutral pH.[15]

With the development of nanotechnology, a major impact on materials science has been noticed. The production of nanomaterials has gained considerable attention for adsorption, catalysis and optical applications, particularly when biomaterials are involved.[16, 17] Nano-hydroxyapatite (nano-HAp) is attracting interest as a biomaterial for its use in prosthetic applications due to its similarity in size, crystallography and chemical composition with those of human hard tissue. Bone and tooth enamel are largely composed of a form of this mineral. The present work focuses on the study of femoral head (the highest part of the thigh bone) samples of different origins (human and bovine) (Fig. 1b-1b') subjected to different calcination temperatures (between 700° and 1100°C), with regard to

*Corresponding author; email: kerimemreoksuz@gmail.com

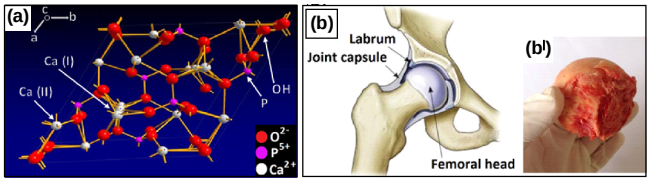


Fig. 1 – (a) Schematic illustration of crystalline structure of hydroxyapatite ($(Ca_{10}(PO_4)_6(OH)_2$), (b) schematic view of the femoral head[17] (b') inset: original head of the human femur extracted after surgery

their influence on chemical and structural properties. Besides the standard characterization techniques, Fourier transform infrared spectroscopy (FT-IR), X-ray diffraction (XRD) and field emission scanning electron microscopy (FESEM) were employed for phase and structure analyses. From the results, some differences were drawn between bovine and human bone samples.

Materials and Experimental Procedure

HAp derived from natural bone (femur diaphysis) of different origins (human and bovine) was obtained under similar processing conditions. Human bone used in this study was biologically inactive femur from donors, supplied by the Medical Faculty Research Hospital, Turkey.[18] The experiments were signed by the Medical Ethical Committee of Medical Faculty Research Hospital, Cumhuriyet University, under permit of MEC-HS(Hu) 2011-362. All patients signed consent for the collection and use of their femoral bones after surgery. Femoral heads were extracted with corkscrew and then hip hemiarthroplasty was applied. The bovine bones were collected from a local butchery. Fresh bones of each specimen were cut into smaller pieces and cleaned well to remove most adhering impurities. Then the bones were boiled in distilled water for 30 min for degreasing and easy removal of tissues and bone marrow. This procedure was repeated twice with fresh water. The bone samples were totally degreased through immersion in an alcohol series (ethanol at 70%, v/v), followed by washing with distilled water. Then they were kept in (NaClO) (30%, v/v) for at least 48 h and were rinsed again. Finally, they were stored in formaldehyde solution (4%, v/ v) at 4°C. Before use, the samples were thoroughly rinsed with distilled water and subsequently dried in a vacuum oven at 60°C for 3 days.[19] Two types of powders were crushed in 250 mL HDPE (high density polyethylene) jars at 300 rpm for 144 h with 5:1 ball to powder ratio in a ball mill. Both the bones were labelled and calcined at 5 different temperatures for SEM-STEM (Tescan® Mira3 XMU, Brno, Czechia), XRD (Rigaku D-Max 2200, Japan) and FT-IR (Bruker TensorII, Alpha ATR, Germany) investigations.

Transmission electron microscope (TEM) module was mounted onto SEM stage to obtain STEM (scanning transmission electron microscopy) on FE-SEM. The operating voltage was 30 kV and the working distance was adjusted to 3 mm to evaluate the sample on Cu grid more accurately. TEM was on the dark field mode to determine the corresponding layer or particle surfaces with higher contrast. In TEM examination, the lighter is the particle, the lower the crystal density occurs. It may also be caused by overlapping of the particles that interfere with the incident beam to be seen darker. An X-ray diffractometer with a monochromatic CuKα radiation (λ=1.5408 Å) was used over a 2θ range from 20° to 60° to characterize the crystal structure of the powder batches, where the diffractograms were compared with the standards complied by the JCPDS (Joint Committee of Phase Diffraction Standards). Average crystallite sizes (D) of the samples were calculated using XRD data and Debye-Scherrer's equation:[20]

$$D = k\lambda/\beta\cos\theta \quad ..(1)$$

where k=0.9 is the shape factor of the average crystallite, λ is the radiation wavelength of CuKα, β is the full width at half maximum (FWHM) of the main diffraction peak and θ is the corresponding Bragg's angle.

FT-IR analyses were carried out in the attenuated total reflection (ATR) unit between 400 and 4000 cm^{-1} and transmittance ratio was evaluated versus the inverse of wave number. The ATR unit provides an ease of direct measurement of powder in front of the optical zone to be detected. Bending, stretching, vibrational modes of molecule bands were discussed.

Results and Discussion

Crystallographic Analysis

The XRD analysis in Fig. 2 shows the increase in intensity which leads to the increase in crystallite size. Peak intensities as also crystallinity are observed to increase with increasing temperatures from 700° to 1100°C. Sharp crystallinity is seen after 900°C with better separation of peaks at different 2θ angles. Figures 2a and 2b represent XRD patterns of bovine bone and human bone, respectively. All XRD patterns were labelled to 09-0432 coded JCPDS file.

The grain refinement for human bone was estimated as 24±3 nm at 700°C with an increased rate of 193±16 nm at 1100°C as illustrated in Fig. 3 by spheroids; the dashed line shows the SEM measurement and regular line shows the XRD grain refinement results. The increasing trend was attributed to the agglomeration via partial sintering of particles and even growth of particles in primary atomic orientations. Similar grain refinement for bovine bone was evaluated as 28±4 nm at 700°C with an increased rate of 224±21 nm at 1100°C as shown in Fig. 3 by diamond symbols. For bovine bone there was a sharp increase in crystallite size from 28 to 96 nm with a regular linear rate while the human bone increased gradually. For SEM measurement case, as seen from Fig. 3 for the right ordinate, the particle size remains constant up to 900°C, then the discrepancy increases due to sintering and hard agglomerate formation by increasing temperature. The particles may lose their single crystal spheroid like form by forming irregular shaped and poly crystal particles. Up to 1100°C, the crystal size increases to 224 nm, while the measurement from SEM image shows

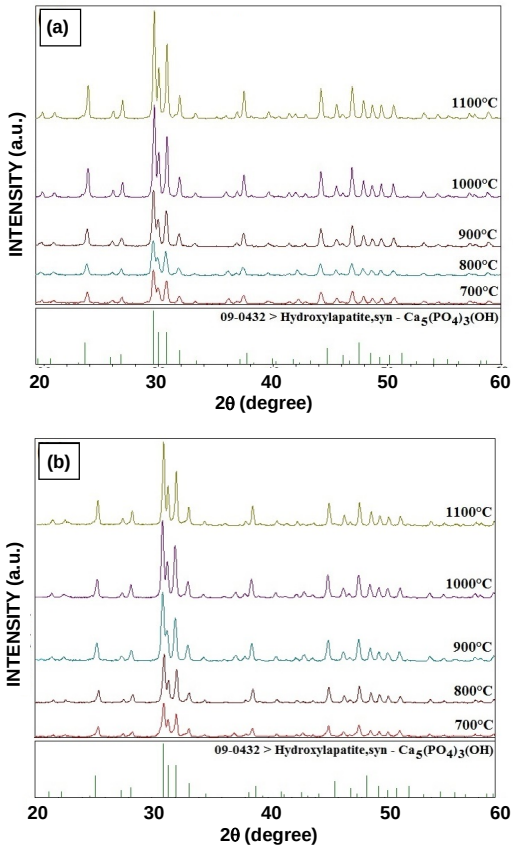


Fig. 2 – XRD patterns of (a) bovine and (b) human bone samples calcined at different temperatures for 2 h

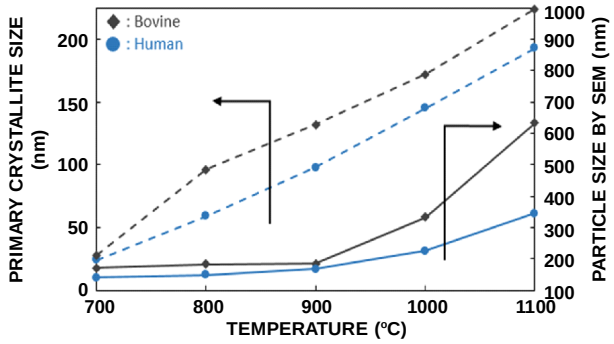


Fig. 3 – Primary crystallite size measurement by XRD grain refinement from Debye-Scherrer formula (dashed lines) and particle size measurement from corresponding SEM images by linear intercept method (regular lines) with respect to temperature

a particle size of 345 nm for human bone and 632 nm for bovine bone. One can say that the increased particle size led to polycrystal formation as seen from the XRD grain refinement analysis, even more polycrystalline forms for bovine bones.

FT-IR Study

Figures 4a and 4b show the FT-IR spectra in the 450-1700 cm^{-1} and 3550-3650 cm^{-1} range of the bovine and human bone samples, respectively before and after thermal treatment at 700°-1100°C for 2 h. FT-IR active

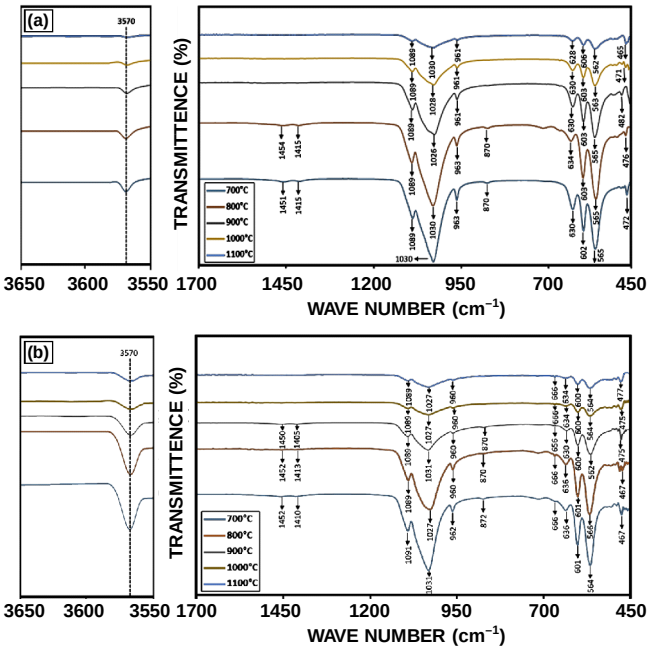


Fig. 4 – FT-IR spectra comparisons of (a) bovine and (b) human bone samples after calcination at 700°, 800°, 900°, 1000° and 1100°C for 2 h

bands were marked with arrows to express the differences between bovine and human bone in detail. The FT-IR spectra of bone powders show a large number of bands corresponding to different stretching/vibrational modes of the same and/or different functional groups. All absorption bands originated by the collagen, viz. at 1540 and 1634 cm^{-1} (and also in the 2800-3500 cm^{-1} region),[21] disappear after calcination at 700°C, which suggests that the organic component has been removed from the bone samples. In addition, most of the bands due to phosphate vibrations of HAp largely decreased in intensity after calcination. This behavior has been described by other authors[22–24] as a consequence of thermal treatment of apatite.

Symmetric stretching and vibrational modes of OH^- occur ~3570 cm^{-1} (left widened region of 3650-3550 cm^{-1}) and 633 cm^{-1}, respectively in the FT-IR spectra of bone powders, calcined in the range of 700°-1100°C.[25] The OH^- peaks tend to get lowered and disappeared (Figs. 4a and 4b), which may be attributed to collagen deterioration by calcination. The human bone withstands the OH^- ions which may be attributed to the interconnectivity of collagen rich 3D network. Weak absorption bands from 1405 to 1454 cm^{-1} are due to the presence of carbonate ions (CO_3^{2-}) which is assumed to be by absorption of atmospheric carbon dioxide during sample preparation. The strongest bands at ~1031 and ~1089 cm^{-1} are due to ν_3 asymmetric stretching of P–O. The decreasing intensity in peaks may be attributed to the presence of total powder after calcination and low absorption percent. The bands observed at ~962 cm^{-1} are due to ν_1 symmetric stretching mode of O–P–O in PO_4^{3-}. The pairs of bands observed at 565/602, 565/603, 565/603, 563/603, 562/606 cm^{-1}, and 564/601, 566/601,

562/600, 564/600, 564/600 cm^{-1} for bovine and human bone powders, respectively are assigned to ν_4 asymmetric bending mode of O–P–O in PO_4^{3-}. The characteristic peaks at 472, 476, 482, 471 and 465 cm^{-1}, and 467, 467, 475, 475 and 477 cm^{-1} for bovine and human bone powders, respectively are due to ν_2 symmetric bending mode of O–P–O in PO_4^{3-}.[25, 26] These results confirm that the chemical composition of human and bovine bone samples is quite similar.

SEM Analysis

Figure 5 shows the SEM secondary electron imaging of powders calcined at five different temperatures; Figs. 5a to 5e (above) shows the bovine bone while Figs. 5a to 5e (below) shows the human bone. It is clear from the SEM pictures that bovine bone calcination from 700° to 1100°C increased the particle size from 171 to 632 nm, similar to the trend seen from the XRD results. Figure 5b shows a different trend in particle size increase than that obtained from XRD analysis result. This discrepancy may be due to the fact that agglomerated particles are measured by SEM, where separate particles' orientations are measured by XRD. Hard agglomerates are formed due to the increase of temperature. In case of human bone calcination from 700° to 1100°C, the slight increase from 140 to 420 nm was measured by counting at least 100 particles from two different pictures of same magnification by linear intercept method. The slower increase in particle size can be attributed to the natural formation of human bone which does not lose its covalent bonded hydroxyl groups with increasing temperature, while in case bovine bone formation the bonding of hydroxyl groups are different and may lose its OH^- with increasing calcination temperature. Hence, the increase in temperature does not deform the structure of OH^- groups in human bone while bovine bone releases OH^- at a wide range of temperature. Somehow, the structure does not decompose mostly and the phase was $(Ca_{10}(PO_4)_6(OH)_2)$ in a regular basis.

STEM Analyses

Since the SEM images of human bone are independent of calcination temperature, the formation of particles after clustering was needed to be evaluated by TEM. Calcination of human bone had finer particle sizes than bovine bone.

In the STEM images of human bone, calcined at 700°-1100°C (Figs. 6a-6e), the particles are of the mentioned dimensions as in XRD crystallite size while the

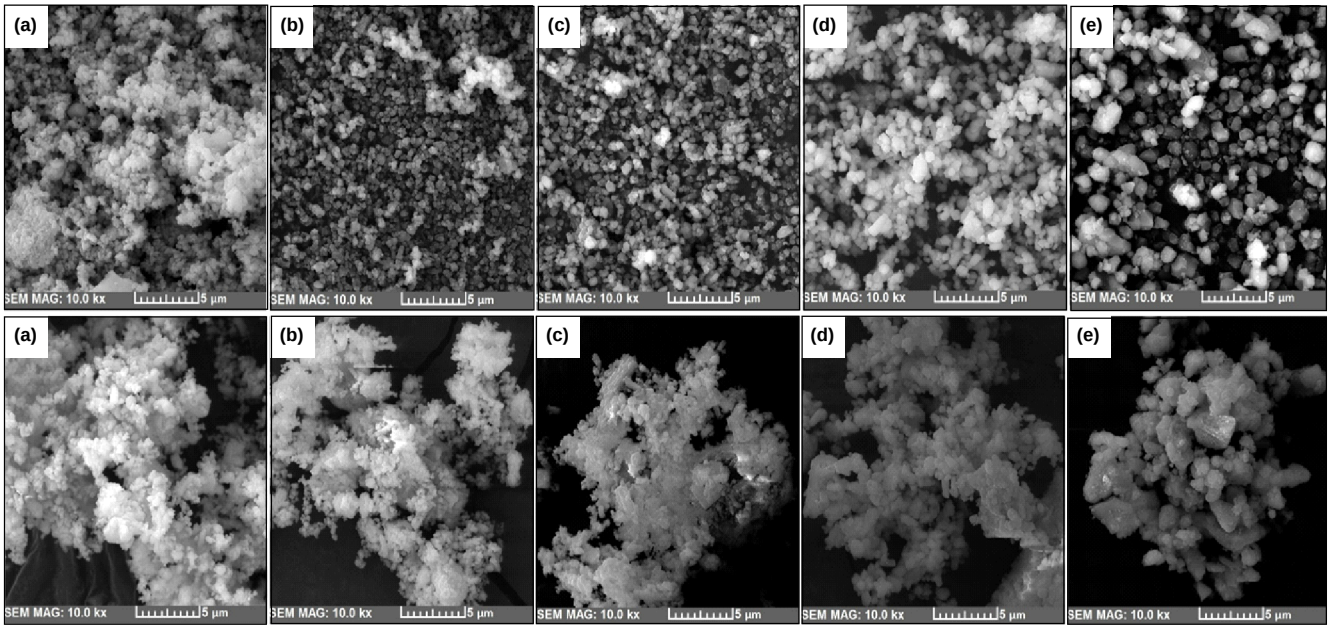


Fig. 5 – SEM images of bovine bone (above) and human bone (below) calcined at: (a) 700°C, (b) 800°C (c) 900°C (d) 1000°C and (e) 1100°C for 2 h

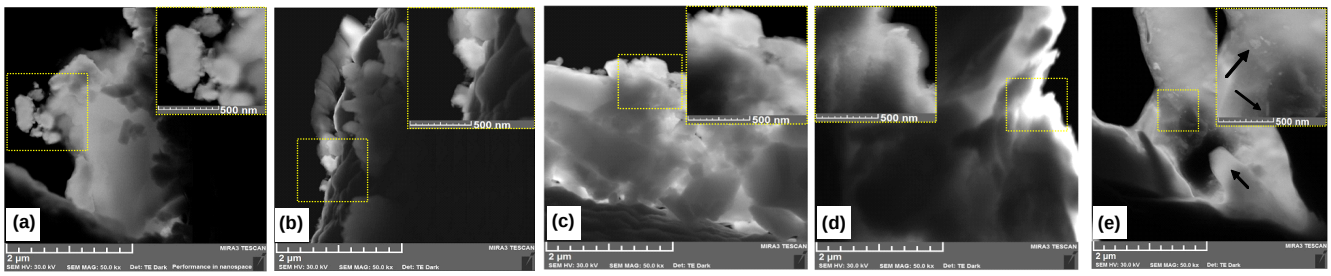


Fig. 6 – STEM images of human bone calcined at (a) 700°C (b) 800°C (c) 900°C (d) 1000°C and (e) 1100°C for 2 h

agglomerated ones are as in SEM measurement. TEM is a useful instrument to measure the initial clusters and agglomerated particle size of HAp as found from XRD and SEM results, respectively. The increasing temperature increased the particle size as illustrated in SEM. After calcination at and above 900°C (Figs. 6c-6e), the clusters got decreased in amount, but the size got larger. From Figs. 6d and 6e, the growth direction of HAp were found to be in c direction. Especially in Fig. 6e the basal plane of agglomerated ($Ca_{10}(PO_4)_6(OH)_2$) particle as well as the finer particles of inset picture were found to be hexagonal and elongated (shown by arrows). Figure 6d can be considered as the beginning of elongated particle formation in lower temperature. The elongated particles as well as hexagonal type basal plane growth of some particles are seen after calcination at 900° to 1100°C.

Conclusions

Following conclusions can be derived from the present study;

- The human and bovine bone powders obtained from natural supplies were produced as nano powders by different calcination temperatures with a great success.
- The calcination was performed at five different temperatures and the powders were characterized by XRD for phase purity and SEM-STEM for particle morphology and size. The powders were analysed to be phase pure HAp nano powders with hexagonal shaped basal elongated particles.
- The bovine bone apatite showed a regular increasing trend for increasing primary crystallite size and powder size characteristics with increasing calcinations temperature, while the human bone apatite showed a sudden increase in primary crystallite size followed by a regular trend for crystallite size found from XRD grain refinement analysis by the Debye-Scherrer. Besides, the FT-IR and XRD results indicated that the human bone has a non-agglomerated structure and the powder size is retained in nano size even at higher temperatures.
- The main reason for the smaller powder size characteristic for human bone can be attributed to the natural collagen distribution in bones while the bovine bone collagen formation was more aggregated and not well distributed between the apatite crystals. The loading conditions of human and bovine bone may also favor the distribution of collagen between the crystals and the feeding procedure must be investigated in further detail.

References

1. R. Murugan and S. Ramakrishna, *Compos. Sci. Technol.*, **65**, 23-35 (2005).
2. S. M. Best, A. E. Porter, E. S. Thian and J. Huang, *J. Eur. Ceram. Soc.*, **28**, 13-19 (2008).
3. J. Chakraborty and D. Basu, *Trans. Indian Ceram. Soc.*, **64**, 171-192 (2005).
4. B. Wenz, B. Oesch and M. Horst, *Biomaterials*, **22**, 1599-1606 (2001).
5. A. B. Khalil, S. W. Kim and Y. K. Kim, *Mater. Sci. Eng. A*, **1**, 368-372 (2007).
6. S. Guizzardi, C. Montanari, S. Migliaccio, R. Strocchi, R. Solmi, D. Martini and A. Ruggeri, *J. Biomed. Res. Appl. Biomater.*, **53**, 227-234 (2000).
7. S. Joschek, B. Nies, R. Krotz and A. Gopferich, *Biomaterials*, **21**, 1645-1658 (2000).
8. R. Murugan, S. Ramakrishna and K. P. Rao, *Mater. Lett.*, **60**, 2844-2847 (2006).
9. K. Haberko, M. M. Buc´Ko, J. Brzezin´Ska-Miecznik, M. Haberko, W. Mozgawa, T. Panz, A. Pyda and J. Zarebski, *J. Eur. Ceram. Soc.*, **26**, 537-542 (2006).
10. R. Murugan, K. P. Rao and T. S. S. Kumar, *Bull. Mater. Sci.*, **26**, 523-528 (2003).
11. G. Wei and M. Px, *Biomaterials*, **25**, 4749-4757 (2004).
12. S. J. Kalita, A. Bhardwaj and H. A. Bhatt, *Mater. Sci. Eng. C*, **27**, 441-449 (2007).
13. N. Y. Mostafa and P. W. Brown, *J. Phys. Chem. Solids*, **68**, 431-437 (2007).
14. S. Teixeira, M. A. Rodriguez, P. Pena, A. H. De and M. P. Ferraz, *Mater. Sci. Eng. C*, **29**, 1510-1514 (2009).
15. L. Guo, M. Huang and X. Zhang, *J. Mater. Sci.: Mater. Med.*, **14**, 817-822 (2003).
16. N. Kantharia, S. Naik, S. Apte, M. Kheur, S. Kheur and B. Kale, *J. Dent. Res. Sci. Dev.*, **1**, 15-21 (2014).
17. I. Cacciotti, "Cationic and Anionic Substitutions in Hydroxyapatite", pp. 145-211 in: *Handbook of Bioceramics and Biocomposites*, Ed. I. Antoniac, 1st edition, Springer, Cham, Switzerland (2016).
18. K. E. Öksüz and A. Özer, *Dig. J. Nanomater. Biostruct.*, **11**, 167-172 (2016).
19. M. Figueiredo, A. Fernando, G. Martins, J. Freitas, F. Judas and H. Figueiredo, *Ceram. Int.*, **36**, 2383-2393 (2010).
20. A. Monshi, M. R. Foroughi and M. R. Monshi, *World J. Nano Sci. Eng.*, **2**, 154-160 (2012).
21. N. Ignjatovic, V. Savich, S. Najman, M. Plavsic and D. Uskokovic, *Biomaterials*, **22**, 571-575 (2001).
22. C. Y. Ooi, M. Hamdi and S. Ramesh, *Ceram. Int.*, **33**, 1171-1177 (2007).
23. S. E. Etok, E. Valsami-Jones, T. J. Wess, J. C. Hiller, C. A. Maxwell, K. D. Rogers, D. A. C. Manning and S. L. Woodgate, *J. Mater. Sci.*, **42**, 9807-9816 (2007).
24. V. K. Mishra, B. N. Bhattacharjee, O. Parkash, D. Kumar and S. B. Rai, *J. Alloy. Compd.*, **25**, 283-288 (2014).
25. V. K. Mishra, S. B. Rai, B. P. Asthana, O. Parkash and D. Kumar, *Ceram. Int.*, **40**, 11319-11328 (2014).
26. V. K. Mishra, B. N. Bhattacharjee, D. Kumar, S. B. Rai and O. Parkash, *New J. Chem.*, **1-3**, 1-11 (2016).